

Q-switched Ti:Er:LiNbO₃ waveguide laser

S. BALSAMO, S. MAIO, I. MONTROSSET

Dipartimento di Elettronica, Politecnico di Torino, 10129 Torino, Italy

H. SUCHE, W. SOHLER

Angewandte Physik, Universität-GH Paderborn, D-33098 Paderborn, Germany

Received 24 March; accepted 24 April 1998

Q-switched operation of a Ti:Er:LiNbO₃ waveguide laser has been achieved with up to 2.4 W pulse peak power (0.18 μJ) at 2 kHz repetition frequency with an intracavity Mach–Zehnder-type amplitude modulator. A theoretical model has been developed to describe the laser operation. Good agreement between numerical and experimental results has been achieved. Significant potential for improvement is predicted.

1. Introduction

In the last few years new selective doping techniques [1, 2] of rare earth ions like Er have been developed, to take advantage of the excellent fluorescence properties of Er-ions in the third telecommunication window which have stimulated a growing interest in Er-doped integrated optical devices, especially lasers. Among the different possible substrates for Er-doped waveguide lasers LiNbO₃ is very attractive [2]. In contrast to vitreous and many other crystalline materials, LiNbO₃ allows the incorporation of Er up to the solid solubility limit without fluorescence quenching [3]. This feature promises, together with the long fluorescence lifetime of the Er-ions, a high storage capability of the excitation energy and waveguide lasers of high power conversion efficiency. This can be exploited for the design of a Q-switched laser of high efficiency. Moreover, due to its excellent electro-optic properties, LiNbO₃ allows the development of lasers with monolithically integrated intracavity modulators for active modelocking [4] and Q-switching [5].

In this paper we report the design, the fabrication and the experimental results of a Q-switched Ti:Er:LiNbO₃ waveguide laser. Parallel to the experimental investigations a model for the theoretical description of Q-switched laser operation has been formulated and a computer code developed. The experimental results are compared to the numerical predictions.

2. Design and fabrication

The laser utilizes a folded intracavity Mach–Zehnder-type intensity modulator as the Q-switch. The corresponding waveguide structure of the laser and the set-up for the experimental investigation of the Q-switched operation are shown schematically in Fig. 1.

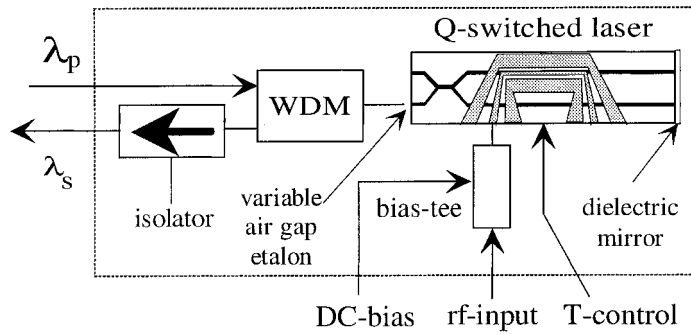


Figure 1 Schematic sketch of the laser structure and the experimental set-up for the investigation of Q-switched laser operation.

The intracavity modulator allows one to control the cavity loss which is the basis for Q-switched laser operation: generating pulses of high peak power. The better the modulator extinction is, the more the stored energy in the active medium grows before pre-lasing sets in.

The actual device has a length of about 57 mm. Half (with respect to the X -direction) of the Z -cut (Y -propagation) LiNbO_3 substrate has been doped near the surface over the complete length by indiffusion of 30 nm of vacuum-deposited Er at 1130°C for 150 h. Subsequently, the photolithographically delineated $6.5\ \mu\text{m}$ wide and 102 nm thick structure of Ti-stripes has been in-diffused at 1060°C during 7.5 h to form the waveguide channels. The part to the right of the splitter is 44 mm long. Attenuation figures of the undoped channels to $0.1\ \text{dB cm}^{-1}$ (TE) and $0.2\ \text{dB cm}^{-1}$ (TM) have been measured at the 1523 nm wavelength, respectively. In the doped waveguides almost the same attenuation figures can be estimated from the difference between the measured transmission and absorption. The FWHM figures of the near field intensity distributions of the modes at the 1556 nm wavelength are $6.8\ \mu\text{m} \times 4.9\ \mu\text{m}$ (width \times depth; TE) and $4.7\ \mu\text{m} \times 2.9\ \mu\text{m}$ (TM), respectively. Within experimental error the intensity distributions are identical for doped and undoped channels. To avoid excess losses of the TM-mode, a $0.6\ \mu\text{m}$ thick insulating SiO_2 buffer was vacuum deposited onto the substrate surface prior to the electrode fabrication.

The electrode structure of the intracavity modulator (Q-switch) is a symmetrical coplanar microstrip line with a gap to hotline width ratio of 0.75. The length of the electrode is about 15 mm. Only a thin electrode has been fabricated by photolithographic lift-off of a sandwich of 30 nm sputtered Ti and 120 nm sputtered Au, since the modulator is operated at low frequency as a lumped device without low resistance termination.

The splitter is a zero gap directional coupler of $190\ \mu\text{m}$ central section length. In TM polarization 56 (47)% of the guided power are routed to the bar state at 1480 (1556) nm wavelength. In TE polarization 91 (94)% are routed to the bar state, respectively.

The laser has a Fabry–Perot cavity comprised of a dielectric mirror and a variable etalon with an air gap. The dielectric mirror has a high reflectance (98%) at both emission wavelength ($\lambda_s \approx 1561\ \text{nm}$) and pump wavelength ($\lambda_p \approx 1480\ \text{nm}$). In this way double pass pumping is provided, allowing an improved pump absorption efficiency. On the other side a variable output/pump coupler mirror has been realized by an adjustable, piezoelectric-

ally driven air gap etalon formed by the endfaces of the pump input/signal output fibre (common branch) of a fibre optic wavelength division multiplexer (WDM) and the polished Ti:Er:LiNbO₃-waveguide endface.

3. Theoretical model

We have developed a dynamic model for a Q-switched laser with an intracavity folded Mach-Zehnder intensity modulator schematically shown in Fig. 1 and described in Section 2.

The branched resonator (see Fig. 1) characteristics are obtained through the approach used in [6], which leads to a resonance condition involving the S-matrix coefficients of the power splitter and the mirror reflectivities. Introducing a time-varying phase shift $\Delta\varphi(t)$ on each branch of the resonator, we can obtain an expression which accounts for the amplitude modulation effect through an equivalent power gain:

$$G = \exp(\tilde{g}L) \{1 - 4S_{13}^2 S_{14}^2 \exp[(g_3 + g_4)l - 2\tilde{g}L] \sin^2 \Delta\varphi(t)\} \quad (1)$$

where $\exp(\tilde{g}L) = (S_{13}^2 \exp(g_3 l) + S_{14}^2 \exp(g_4 l))$, l is the length of the two right branches of the resonator, which have gain g_2 and g_3 , respectively, and L is the total cavity length (see Fig. 1). The S -parameters refer to a concentrated power splitter, with port 1 as the pump/output port and the two ports to the right are denoted as 3 and 4. S_{13}^2 and S_{14}^2 are the transmission coefficients, as defined in [6].

The temporal variation of the equivalent power gain can be considered as a variation of the cavity losses, which has been introduced in the field equations.

In our model the Er:LiNbO₃ system has been considered as a quasi-2-level system, and the laser cavity dynamics is described through a mean field set of rate equations for the various parts of the cavity [7]. The optical field is described with the multimode longitudinal mean field approach, which yields a system of coupled differential equations for the longitudinal modes of the cavity and for the pump power dynamics.

Summarizing, we have a system of $N_{\text{mode}} + 4$ coupled equations, N_{mode} for the longitudinal modes, one for the pump and one for the upper level population density in each section of the active medium.

Due to the very different time constants of the atomic system and of the optical field, the system is strongly stiff. The numerical integration by means of an IMSL [8] routine with adaptive time step for stiff systems was suitable for overcoming the numerical difficulties.

4. Experimental and numerical results

Using a pigtailed high power laser diode as the pump source a cw threshold of about 58 mW was achieved for σ -polarized emission at 1561 nm wavelength in the high Q-state of the cavity. The numerically calculated threshold is about 54 mW. No π -polarized emission could be achieved although the intracavity modulator had been optimized for a high extinction ratio (symmetric power splitting) in this polarization. The extinction ratio in σ -polarization is very low. 1.1 dB was calculated from the measured splitting ratio (see Section 2.). For operation of the Q-switched laser in σ -polarization 80 (20)% of the pump power was adjusted to TE(TM)-polarization yielding optimized operation of the laser.

In Fig. 2 first experimental results of Q-switched operation of the Ti:Er:LiNbO₃ laser for 100 mW incident pump power (left diagram) and the corresponding numerical simulations (right diagram) are presented. Both the drive voltage for the intracavity electro-optic switch and the laser output are shown as a function of time. After switching to the

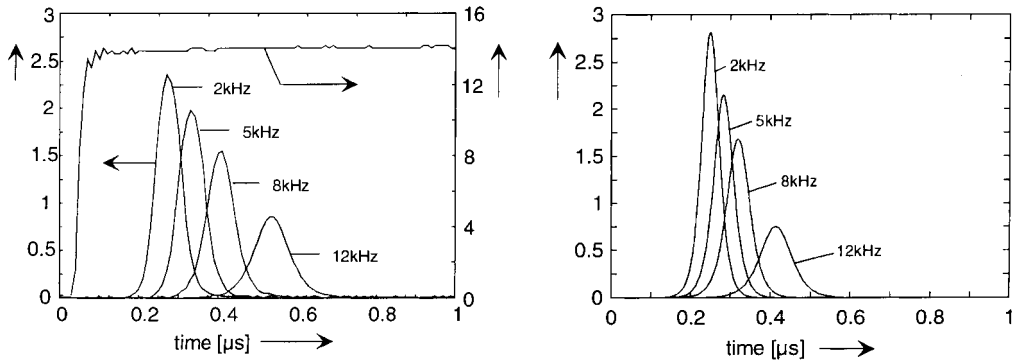


Figure 2 Measured (left diagram) and numerically calculated (right diagram) output power of a Q-switched Ti:Er:LiNbO₃-waveguide laser versus time. Left diagram, right ordinate: measured voltage to drive the intracavity amplitude modulator. Parameter of the set of graphs is the pulse repetition frequency of the Q-switched laser.

higher cavity Q, pulses of up to 2.4 W peak power and up to 0.18 μJ pulse energy are emitted at 2 kHz repetition frequency. At lower repetition rates the pulse peak power decreased again due to the onset of pre-lasing. With increasing frequency the pulses become broader, the peak power is reduced and the pulse build-up-time is increased.

For the simulations we assumed the fabrication parameters as given in Section 2 and the experimentally determined operation conditions given above. The phase bias of the intracavity Mach-Zehnder modulator and the effective reflectivity of the air gap etalon have been varied as fitting parameters.

The results of the numerical simulations agree well with the experimental ones in terms of peak power and pulse width. Moreover, for the same operation wavelength, even better results are predicted assuming an intracavity switch of symmetric power splitting and hence of ideal extinction ratio (see Fig. 3). A maximum peak power of 258 W and a FWHM pulse width of about 7.5 ns is predicted for 55% output mirror reflectivity and a 7 cm long cavity (which is the maximum length compatible with 3 inch wafer technology).

5. Conclusion

We reported to our knowledge the first comparison of experimental and simulation results for Q-switched operation of a Ti:Er:LiNbO₃ waveguide laser. A good almost quantitative agreement between experimental and numerical results was obtained. The peak power of the actual laser was limited by the onset of pre-lasing due to the low extinction ratio of the Q-switch for the TE-polarized operation of the laser. Simulation results predict a high potential for improvements with an optimized laser structure. Pulse peak power levels in excess of 250 W seem to be feasible with 100 mW of incident pump power. With higher pump power levels and at lower repetition rates even higher peak powers and smaller pulse widths are expected (see also [9]).

Acknowledgements

We gratefully acknowledge the support of this work by the European Union within the project ‘Advanced Optical Waveguide Components and Systems’ of the HCM network program and by the ‘Vigoni Program’ funded by DAAD (Germany) and CRUI (Italy).

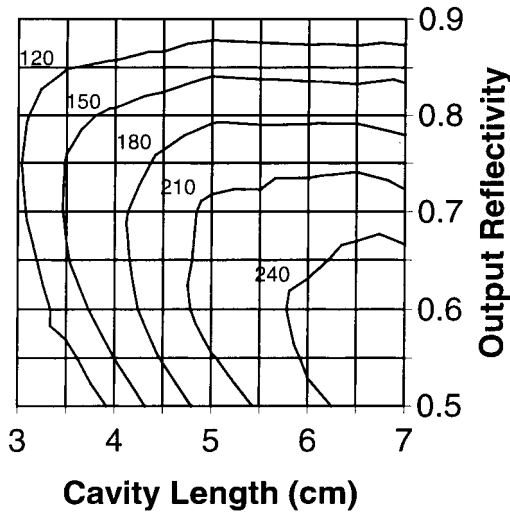


Figure 3 Peak power as a function of cavity length and output reflectivity for an interferometric switch with symmetric power splitting, for 100 (95) mW of incident (coupled) pump and 2 kHz repetition frequency.

References

1. W. SOHLER and H. SUCHE, European Patent No. 0569353 and US Patent Application Serial No. 08/094,199.
2. I. BAUMANN, L. BECKERS, CH. BUCHAL, R. BRINKMANN, M. DINAND, TH. GOG, H. HOLZBRECHER, H. FLEUSTER, M. MATERLIK, K. H. MÜLLER, H. PAULUS, W. SOHLER, H. STOLZ, W. VON DER OSTEN and O. WITTE, *Appl. Phys. A*, **64** (1997) 33.
3. M. FLEUSTER, C. BUCHAL, E. SNOEKS and A. POLMAN, *J. Appl. Phys.* **75** (1994) 173.
4. H. SUCHE, I. BAUMANN, D. HILLER and W. SOHLER, *Electron. Lett.* **29** (1993) 1111.
5. E. LALLIER, D. PAPILLON, J. P. POCHOLLE, M. PAPUCHON, M. DE MICHELI and D. B. OSTROWSKY, *Electron. Lett.* **29** (1993) 175.
6. E. MWARANIA and J. WILKINSON, *IEEE J. Quantum Electron.* **10** (1992) 1700.
7. M. DINAND and W. SOHLER, *IEEE J. Quantum Electron.* **30** (1994) 1267.
8. IMSL Math/Library, Fortran Subroutines for Mathematical Applications, version 1.1 (1989).
9. D. L. VEASEY, J. M. GARY, J. AMIN and J. A. AUST, *IEEE J. Quantum Electron.* **33** (1997) 1647.